Title

Unravelling the Metastable Nature of the Single Site Tungsten Hydride Metathesis Catalyst Supported on γ-Alumina from First Principles

Journal

The Journal of Physical Chemistry C, 123(2)

ISSN

1932-7447

Authors

Joubert, Jérôme
Delbecq, Françoise
Sautet, Philippe

Publication Date

2019-01-17

DOI

10.1021/acs.jpcc.8b09876

Peer reviewed

Unravelling the Metastable Nature of the Single Site Tungsten Hydride Metathesis Catalyst Supported on γ-alumina from First Principles

Jérôme Joubert[†], Françoise Delbecq[†], Philippe Sautet[†&ç]*

†Univ Lyon, ENS de Lyon, CNRS, Université Lyon 1, Laboratoire de Chimie UMR 5182, F-69342, Lyon, France

&Department of Chemical and Biomolecular Engineering, University of California, Los Angeles, Los Angeles, CA 90095, United States

çDepartment of Chemistry and Biochemistry, University of California, Los Angeles, Los Angeles, CA 90095, United States

*corresponding author: sautet@ucla.edu

Abstract

We explore the structure and formation mechanism of the surface tungsten hydride complex supported on alumina, which is a catalyst for alkane and alkene metathesis and cross-metathesis. We show that the kinetics for the formation reaction of the hydride from the grafted alkylidyne-alkyl W complex strongly favors the creation of a metastable W^{VI} tri-hydride, which is less coordinated by the alumina surface than the most stable isomer. The reaction network for the hydride formation involves hydrogenation of the W≡C or W=C bond, hydrogenolysis of W-C bonds, and a second grafting step. The creation of metastable surface complexes is proposed be a key path for the design of active and selective catalysts.

1- Introduction

The rupture and formation of C-C bonds is a fundamental reaction in Chemistry, and metathesis and cross-metathesis reactions are elegant and efficient processes. Since its discovery ten years ago [1,2,3], a very active catalyst based on a tungsten hydride complex supported on γ-alumina (W-H/Al_2O_3) has been successfully used in alkane and alkene metathesis and cross-metathesis.[4,5,6,7,8] It has been proven both experimentally and theoretically that the grafting of the tungsten neopentyl-neopentylidyne [W(≡CtBu)(CH_2tBu)$_3$] complex on γ-alumina initially gives the monografted alkyl-alkylidyne tungsten surface complex [(Al_sO)W(≡CtBu)(CH_2tBu)$_2$] (**1**, Scheme 1).[9] The reaction of this complex with hydrogen generates the active grafted tungsten hydride catalyst. However, the characterization of this tungsten-hydride species is still speculative. Experimentally, the hydride has not been isolated but an IR spectrum has been recorded after treatment of **1** under H_2.[2,3] The purpose of the present work is to characterize the hydride species by means of calculations based on density functional theory (DFT) and to study the mechanism leading to its formation. Grafted W hydrides form an important class of metathesis catalysts that has been later extended to a silica support.[10,11]

2- Methods

The calculations were performed in the framework of density functional theory (DFT) with the PW91 functional[12] using a periodic description of the system as implemented in the VASP code.[13,14] The atomic cores have been described with the projected augmented wave (PAW) technique.[15] The "soft" version of the O atom PAW, with an atomic radius of 1.9 bohr was determined to be sufficient for the study, allowing us to limit the plane-wave energy cutoff to 275 eV. Tests with a harder O atom PAW and the associated plane-wave energy cutoff of 400 eV only decrease the energy difference between the most stable hydride structures by 0.1 eV,

which is smaller than the general error linked with the DFT exchange correlation functional. Brillouin zone integration is converged with a 331 k-point mesh generated by the Monkhorst-Pack algorithm. Minimum energy pathways have been found using the nudged elastic band (NEB) method with eight equally spaced images along the pathway.[16,17] The transition state structures have been fully optimized and characterized by a single negative force constant along the reaction pathway. Vibrational frequencies have been calculated in the harmonic approximation by a numerical evaluation of the Hessian matrix.

The bulk model used for γ-alumina comes from a previous theoretical study of the dehydration of boehmite, with the constraint of a distribution of 25% tetrahedral and 75 % octahedral Al atoms.[18] The (110) surface has been considered since it is the most abundant one on the alumina nanoparticles (~75% of the total surface), and it has been modeled by a 8.4 x 8.1 $Å^2$ periodic slab, composed of 4 layers. The two bottom layers of the slab were maintained in the geometry of the bulk, while the two upper layers were relaxed. Following the alumina preparation procedure, the upper surface is partially hydroxylated, and hence for a realistic modeling a few water molecules should be chemisorbed.[19, 20] For the given cell size, the adsorption of three water molecules represents well the diversity of OH groups seen in IR spectra.[9] It corresponds to a OH coverage of 7.3 OH/nm^2 on the (110) surface or 5.5 OH/nm^2 on the alumina particle, since the main other surface (100) does not present any OH. This coverage is higher than the average value measured for a typical pretreatment temperature of 500 °C (2-4 OH/nm^2)[21,22,23,24] and corresponds to an hypothesis where the surface hydration is not homogeneous, as observed by Métivier et al.[25] These OH group are crucial sites for the grafting on the W complex on alumina. Surface aluminum atoms have a coordination ranging from IV to VI and interact with one or two OH groups. The surface unit cell present one 4-coordinated Al (Al_{IV}), and three five coordinated one (Al_V), including OH or water adsorbates in this coordination count. Key OH groups on the surface for the complex grafting are a

terminal OH on Al_{IV}, a bridging OH on two Al_V and a terminal OH on Al_V. We will show that the choice of OH group for the complex grafting step has a strong influence in its stability and reactivity. In the paper, oxidation numbers will be mentioned by exponent (W^{VI} for example means W at the oxidation degree 6) and neighbor coordination by a subscript (Al_{IV} means 4-coordinated Al).

3- Results and discussion

1-Initial grafted complex and formation of various tungsten hydrides

The formation of complex **1** involves the grafting of $[W(\equiv CtBu)(CH_2tBu)_3]$ on the 4-coordinated $(OAl)_3Al_{IV}OH$ surface atom, hence a tetrahedral surface atom. An $(OAl)_3Al_{IV}$-O-W bond is formed, a neopentane molecule is released and a surface OH group is consumed. The resulting surface species **1** is shown on scheme 1. From this starting point, the possible tungsten hydride species grafted on alumina were thoroughly explored, keeping the Al_{IV}-O-W linkage between the metal and the alumina surface. For the calculations, the heavy tertio-butyl and CH_2tBu substituents have been replaced by methyl groups, as in our previous studies. The model starting complex **1m** reads now $[(Al_sO)W(\equiv CCH_3)(CH_3)_2]$ and is depicted in Scheme 1.

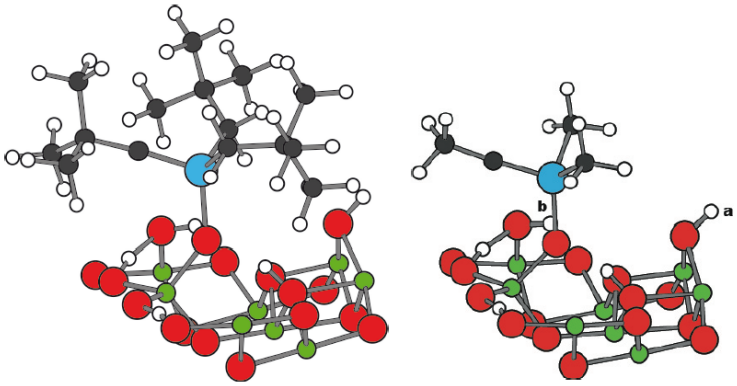

Scheme 1: Grafted alkylidyne-alkyl W complex **1** $[(Al_sO)W(\equiv CtBu)(CH_2tBu)_2]$ on the left ; Model complex **1m** $[(Al_sO)W(\equiv CCH_3)(CH_3)_2]$ on the right. H_a and H_b are involved in the formation of **2** and **2'**, respectively.

The grafted W hydrides have been systematically constructed, assuming that hydrogenolysis or grafting was removing all three ligands on **1** (or **1m**). We will first focus on the stability of these hydrides and in a second step we will explore the formation pathways for the most stable structures. They were sorted in five classes, depending on the number of H atoms on W, from two to four, and on the oxidation degree of the tungsten atom. We have considered W^{VI} complexes and, since equivalent d^2 Ta hydride exist, we have also generated W^{IV} supported hydrides (except for the tetrahydrides). The five classes are hence: W^{IV} dihydride, W^{VI} dihydride, W^{IV} trihydride, W^{VI} trihydride and W^{VI} tetrahydride. The corresponding 13 calculated species are represented in figure 1 and labeled **H1** to **H13**. These labels are only used for the study of the structure and stability of grafted W hydrides. The two most stable structures will be **renumbered** at the end of this section for the exploration of their formation pathways.

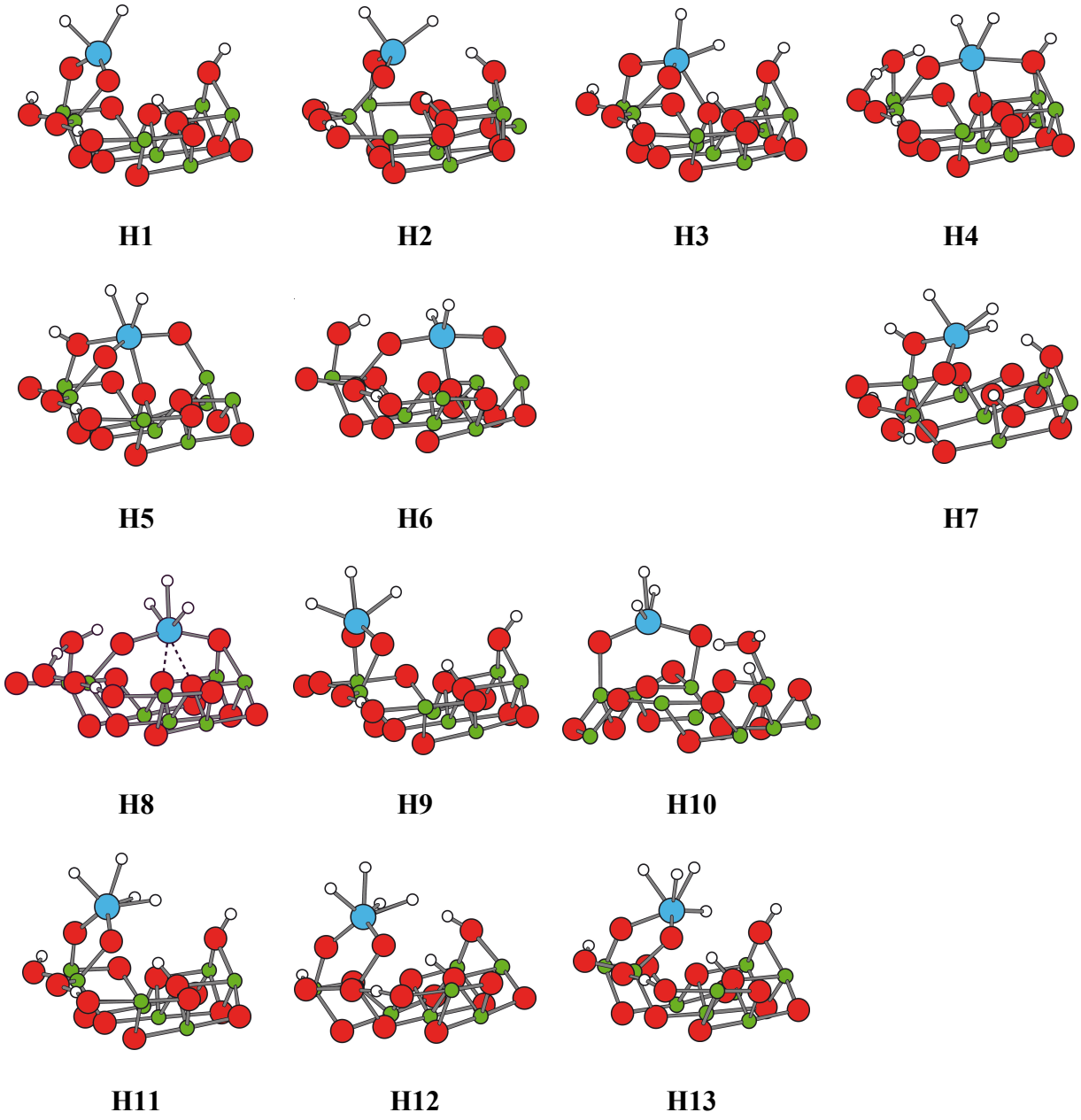

Figure 1: Calculated structure of the W-hydrides grafted on γ-alumina. **H1-H4**: W^{IV} dihydrides; **H5-H6**: W^{VI} dihydrides; **H7**: W^{IV} trihydride; **H8-H10**: W^{VI} trihydrides; **H11-H13**: W^{VI} tetrahydrides.

These grafted hydrides are all neutral. Indeed, it has been impossible to find hydrides with charge separation, as it was the case for zirconium hydrides.[26] Dihydrides **H1-H4** are grafted to the oxide support through two covalent Al-O-W bridges, named as bi-grafted here. Two OH groups have been transformed in this bi-grafting and 4 protons out of 6 remain on

the surface in H_2O or OH groups. These bi-grafted dihydride complexes correspond to W^{IV} species (note that dative W-O bonds can also be formed from donation of oxygen lone pair into vacant W orbitals, but there do not change the W oxidation state). **H1** and **H2** only differ by the orientation of the OH group bridging two surface Al atoms, while **H1** and **H3** only differ by a supplementary dative O-W interaction in **H3** due to a tilting of the O-W-O plane. In **H1**-**H3** the second grafting uses an OH group on one type of surface Al_V via H_b (Scheme 1) while in **H4**, the second grafting is performed via a bridge OH (H_a) on two surface Al_V atoms, slightly further away from the initial Al_{IV} grafting site compared to H_b. Note that the ML_4 W^{IV} d^2 dihydride complexes (**H1**-**H2**) give a calculated distorted tetrahedral structure, and are not stable in a square-planar like arrangement. This contrasts with the case of the tetra phenoxide W^{IV} complexes which are square planar, and can be explained by the absence of π bonding effect from the hydride ligands.[27] Starting from **H4** to form **H5** and **H6**, 2 H atoms are removed from the surface and replaced by a gas phase H_2. Through this process the surface is formally oxidized, and since Al cannot change oxidation number, W^{IV} is transformed into W^{VI}. The tungsten remains bigrafted. Complexes **H7** to **H10** are trihydrides. In **H7** the trihydride complex is only monografted and W has the oxidation degree IV. In **H8**, W is trigrafted with 3 protons remaining on the surface. The trigrafted W trihydride has hence the oxidation degree VI. In **H9** and **H10**, WH_3 is only bigrafted, but instead of the normal count of 4 remaining H on the surface, only 3 H are present. Compared to **H1** and **H4** one proton from a surface OH group is transformed in a hydride on W, hence insuring the formal W^{VI} oxidation state. **H9** and **H10** differ by the O atoms involved in the grafting. Finally, **H11**-**H13** are bigrafted tetrahydrides complexes with 4 protons left on the surface. W is hence at the oxidation degree VI. **H11** and **H12** only differ by the orientation of the bridge OH group, while **H11** and **H13** differ by the orientation of the hydrides.

The relative energies of these grafted hydrides on γ-alumina are compared in Figure 2 (H_2 molecules have been added to keep the same number of H atoms).

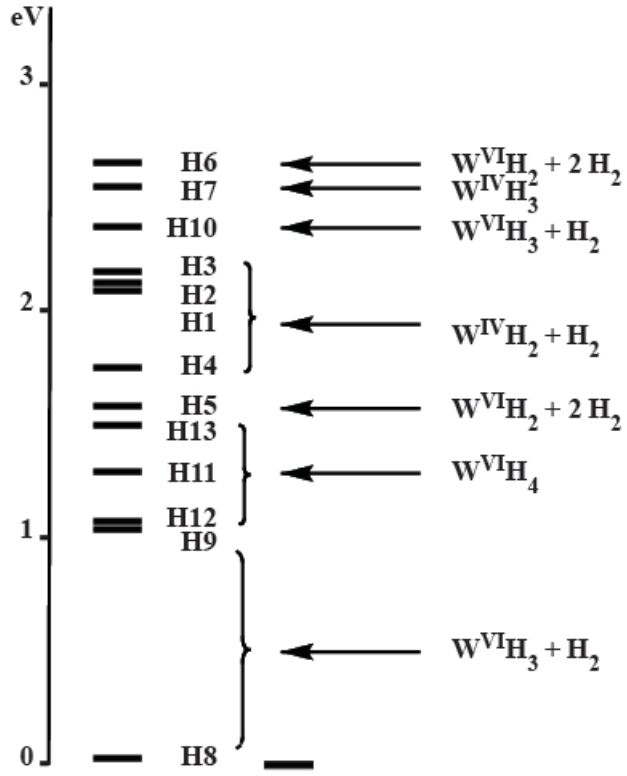

Figure 2: Relative energies of the various grafted W hydrides. Gas phase H_2 molecules have been added to keep the same number of H atoms.

The surface hydrides of W^{IV} are higher in energy compared to those of W^{VI}, two exceptions being **H6**, a W^{VI} complex that distorts the surface tetrahedral Al center and is hence poorly stable, and **H10**. Moreover, the W^{IV} dihydrides can easily be transformed to W^{VI} tetrahydrides by facile oxidative addition under H_2. Hence their probability of existence is very small. A trihydride of W^{VI} **H8** is far more stable than the others: it is depicted with more details in Scheme 2 and will be labeled as structure **2** in the remaining of the article. In this complex, the tungsten atom is bound to the surface by three aluminoxy ligands (one O-Al_{IV} and two O-Al_{VI}) and an aluminoxane bridge (O-μ_2-Al_V,Al_V) and is quasi symmetrical. Hence W occupies the position of an octahedral Al in the alumina network, which contributes to the

high stability. A hydrogen bond clearly exists between one H and a surface hydroxyl (2.02 Å), which further stabilizes the structure.

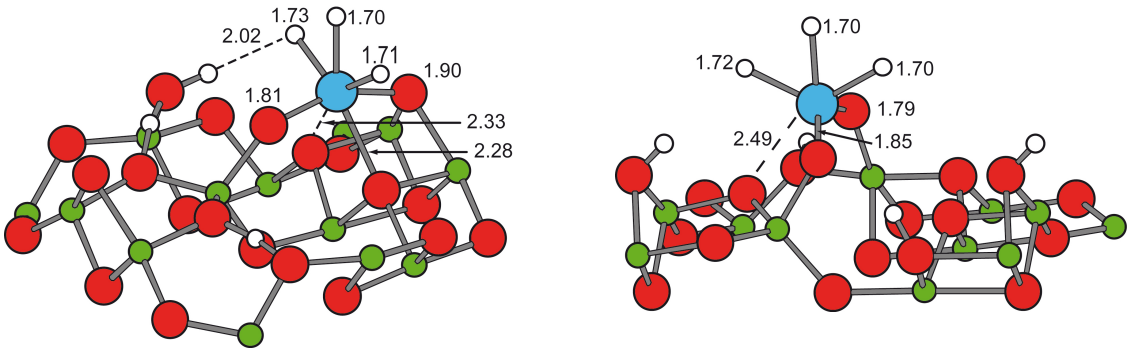

2 **2'**

Scheme 2: Structure of the most stable trihydrides of W^{VI}: **2** (**H8**) on the left; **2'** (**H9**) on the right. Distances in Å.

All attempts to displace a hydride from W to Al, accompanied by a charge transfer forming a cationic W center and an anionic Al as it was seen in the case of Zr grafted complexes,[18] have given highly unstable systems. The formation of Al hydride by spill-over is hence excluded on this support. The experimentally observed Al hydrides are hence linked with a direct reactivity of H_2 on alumina.

We have seen in the introduction that the tungsten hydrides, whatever their nature, are very active in metathesis. In the case of ethylene reactant for example, the first step is its coordination on W. All attempts to coordinate ethylene on **2** failed. The reason is that W is saturated and too deeply inserted in the alumina network. In contrast, the coordination was possible on **H9**, the second most stable complex, also a W^{VI} trihydride. The metastable complex **H9** is hence considered as a prototype of active site for W hydrides on alumina. It is shown in more details on scheme 2 and will be called **2'** in the following. Among the two W-O bonds, one is short (1.79 Å) and it can be viewed as a tungsten-oxo W=O bond in

interaction with the alumina surface. This surface complex can hence be described as a W-oxo-trihydride.

The experimental IR spectrum shows two bands at 1804 and 1903 cm^{-1}.[2] These bands are however rather broad (full width at half maximum ~70 cm^{-1}). The calculated W-H frequencies for the six most stable grafted W hydrides of Figure 2 are given in table S1 in the supporting information. Calculated frequencies are shifted too higher value compared to experiment by ~100 cm^{-1}.[28] The stable trihydride structures **2** and **2'** give three frequencies, but after convolution with a Gaussian to reproduce the experimental broadening, the two highest value combine in one peak. Weak H-bond interaction between some W-H and a surface hydroxyl shifts the low frequency even lower. The reproduction of the separation between the two bands hence depends on the specific distribution of OH groups on the alumina surface, which is not possible to obtain accurately from our necessarily simplifying model of an otherwise rather heterogeneous distribution of OH groups. Hence, due to the limited resolution, the experimental spectrum is completely compatible with the proposed most stable structures 2 and 2'. Therefore, as a first conclusion, the structure of the active W hydride is likely to be a trihydride.

In the next section, we will describe the formation pathways of the two bigrafted hydrides **2** and **2'** starting from the mono-grafted complex **1** and reacting it with H_2. We will see that the path towards **2** is unfavorable in the early steps, and hence the catalyst synthesis process will mainly lead to the formation of the species **2'**.

2- Formation of $W(H)_3/Al_2O_3$ under H_2.

Under H_2 three types of reactions can occur for the surface W alkylidyne-dialkyl complex **1** as shown on Figure 3 for the model complex **1m**. The first one (indicated by

$-CH_4$) consists in a second grafting process on a neighboring surface hydroxyl with elimination of a molecule of methane (experimentally neopentane).

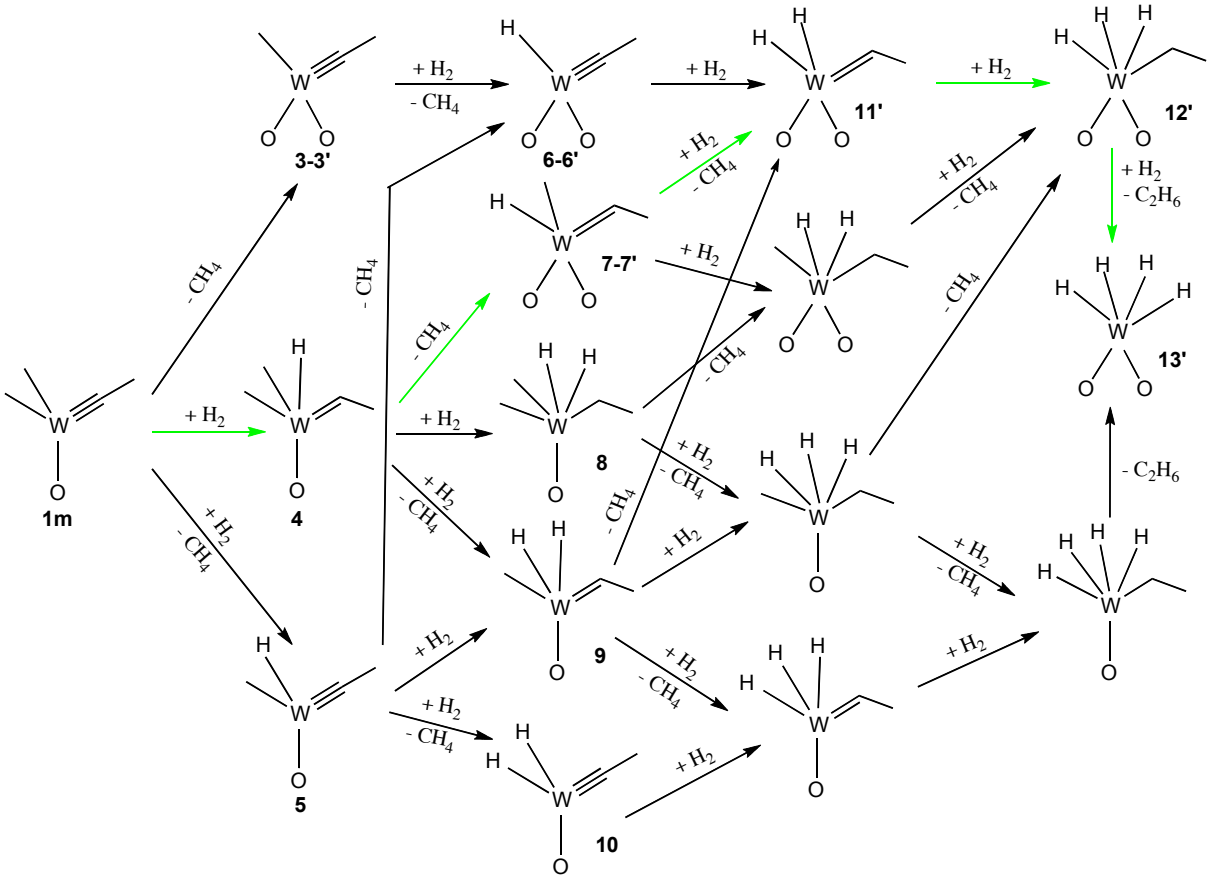

Figure 3: reaction network for the formation of grafted W hydrides on alumina starting from a grafted alkylidyne-alkyl complex. $-CH_4$ (or $-C_2H_6$) indicates a grafting process through an alkyl ligand, $+H_2$ a hydrogenation of the W≡C or W=C bond and $+H_2/-CH_4$ (or $+H_2/-C_2H_6$) a hydrogenolysis of a W-C bond. Green arrows indicate the kinetically preferred pathway.

The second one is the addition of H_2 on the W≡C triple bond, (indicated as $+H_2$) leading to an alkylidene-hydride or in a second step to an alkyl-hydride product. The third one is a hydrogenolysis of a W-alkyl bond (indicated by $+H_2/-CH_4$) with also elimination of methane (neopentane). The key difference between the trihydrides **2** and **2'** resides in the Al-OH site for the second grafting. For **2**, the second grafting takes place on the bridge hydroxyl between two Al_V centers (H_a in Scheme 1), while for **2'**, the hydroxyl involved is singly bound to an Al_V (H_b in Scheme 1). Hence, two pathways must be considered, depending on the site of the

second grafting. The numbers indexed with a prime will correspond to the second grafting on O-Al_{IV} forming intermediates ultimately leading to **2'**.

One of these three elementary reactions (grafting, hydrogenation, hydrogenolysis) can in principle proceed on **1m**, and the formed intermediate complexes can react again following the same type of steps, giving the potential reaction network of Figure 3 that leads to a bi-grafted tetrahydride **13** or **13'**, similar to **H11** or **H13**. This network is complex but only the lowest energy path is relevant. Hence we have focused at each step on the most favorable reaction. The corresponding energy profile for the first two steps is shown in Figure 4 while the structures of the 16 calculated intermediate complexes are given in Figure 5. For each step shown in Figure 4, the transition state (TS) has been characterized and its structure is shown in Figure 6.

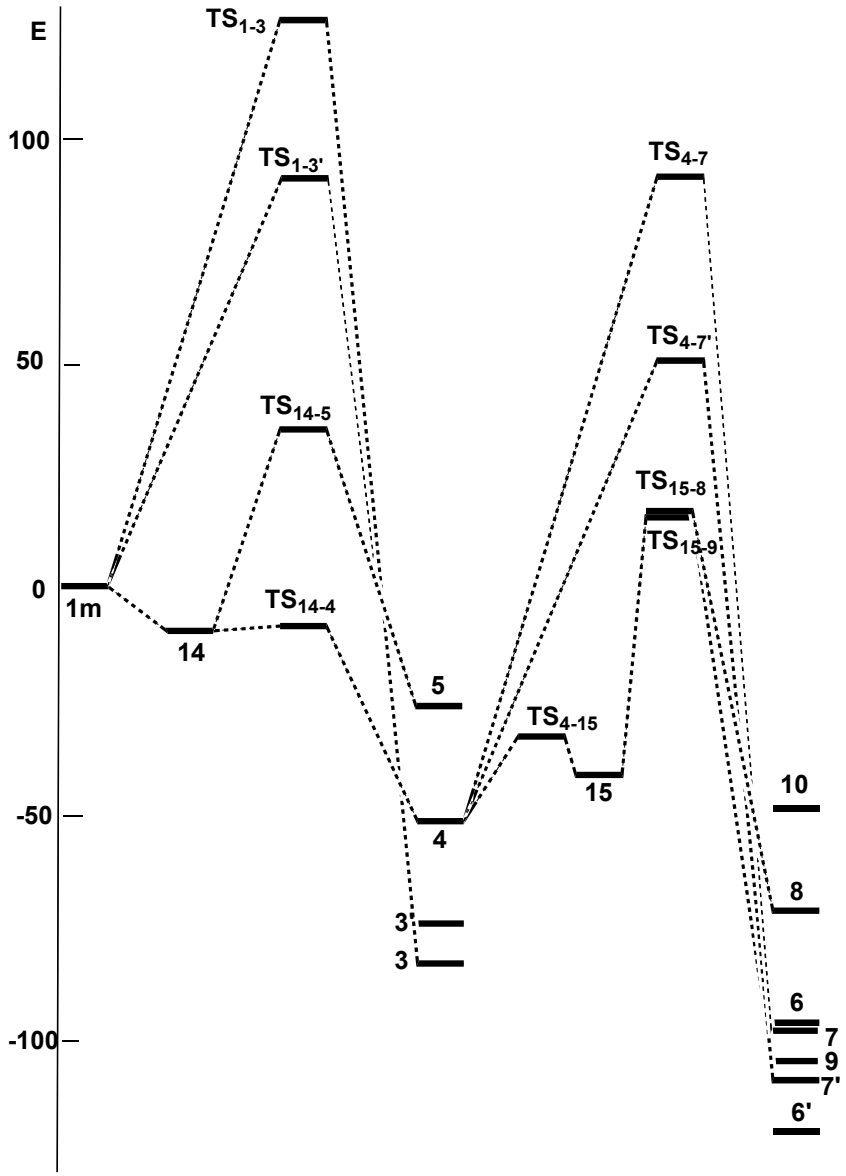

Figure 4: Energy profile (in kJ.mol^{-1}) for the initial part of the reaction network for the formation of grafted W hydrides on alumina shown in Figure 5. Structures 14 and 15 correspond to the molecular adsorption of H_2 on 1 and 4, respectively.

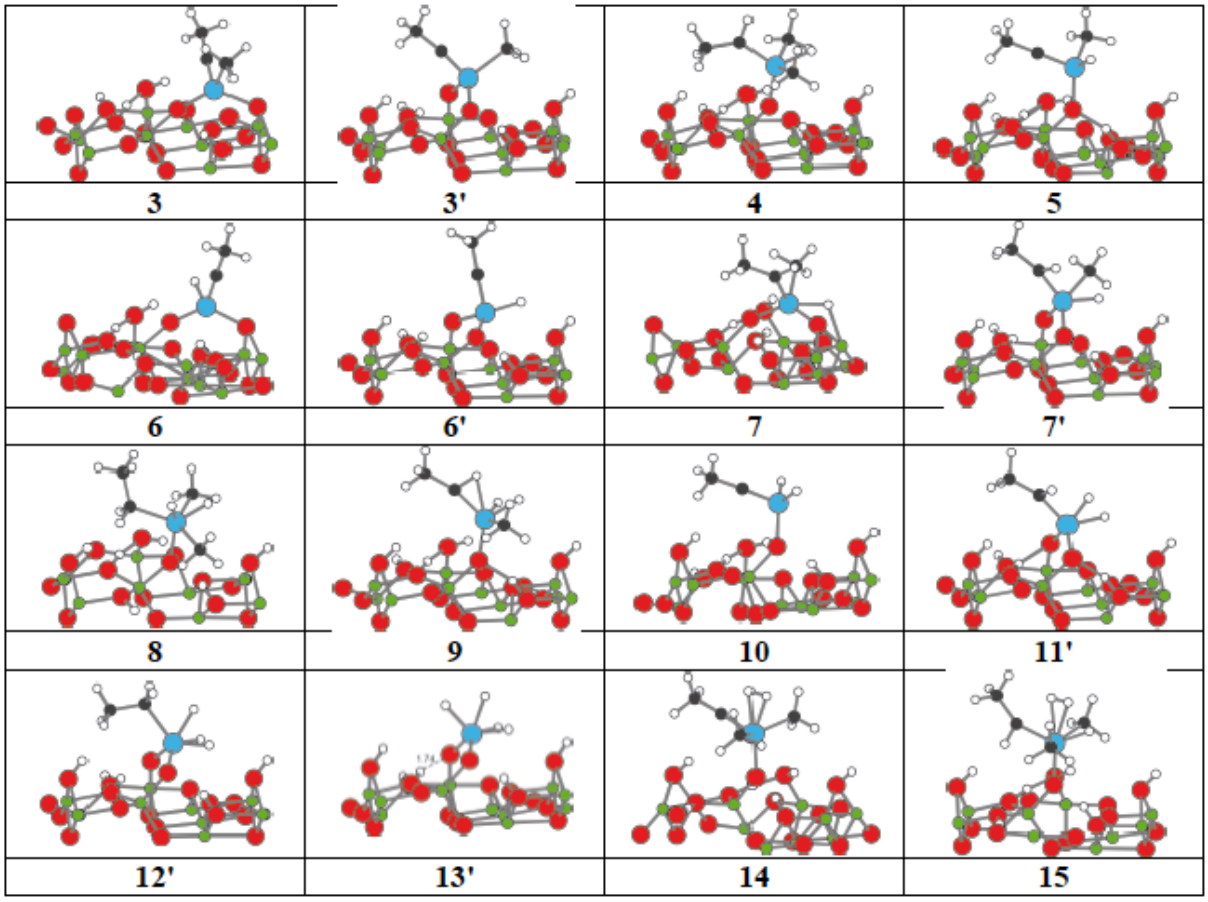

Figure 5- Structures of the intermediates involved in the initial part of the transformation of the methyl-methylidyne tungsten surface complex $[(Al_sO)W(\equiv CMe)(Me)_2]$ **1m** to the tetrahydride $[(Al_sO)_2WH_4]$ **13'**.

Starting from **1m**, the second grafting gives $[(Al_sO)_2W(\equiv CCH_3)(CH_3)]$ **3** and **3'** with a favorable reaction energy of -83 and -74 kJ/mol, respectively. The corresponding activation energies are however very different: a high value (126 kJ/mol) is found for the path through $\mathbf{TS_{1\text{-}3}}$ while a much more moderate barrier (90 kJ/mol) is obtained through $\mathbf{TS_{1\text{-}3'}}$, respectively. Hence, the bi-grafted complex **3** is more stable than **3'** by 9 kJ/mol, but its formation is much slower with a difference in the activation energies of 36 kJ/mol, which at the reaction temperature of 150 °C corresponds to a rate $2*10^4$ slower. The addition of hydrogen on W≡C in **1m** gives $[(Al_sO)W(=CHCH_3)H(CH_3)_2]$ **4** with a reaction energy of -51 kJ/mol. It starts

with the coordination of H_2 at the tungsten atom leading to the complex $[(Al_sO)W(\equiv CCH_3)(H_2)(CH_3)_2]$ **14** with a stabilization of -9 kJ/mol and an activation energy of circa 19 kJ/mol.

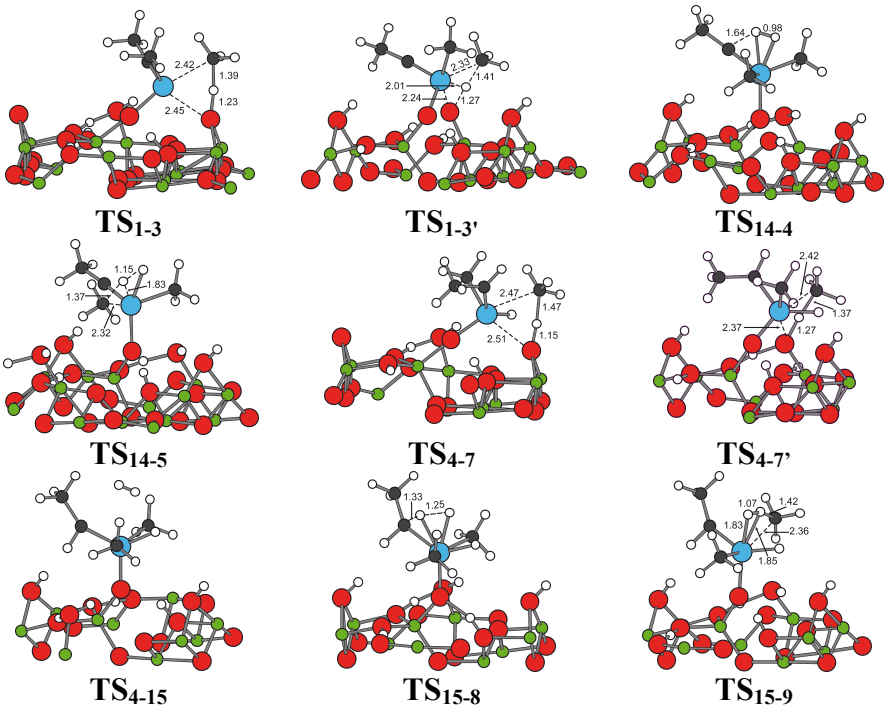

Figure 6- Structures of the transition states involved in the transformation of the methyl-methylidyne tungsten surface complex $[(Al_sO)W(\equiv CMe)(Me)_2]$ **1** to the tetrahydride $[(Al_sO)_2WH_4]$ **13'**.

Then the hydrogenation of the triple bond is very easy through $\mathbf{TS_{14\text{-}4}}$, with an activation energy of only 2 kJ/mol. The third possible reaction occurring at **1m** is the hydrogenolysis with elimination of methane and formation of the $[(Al_sO)W(\equiv CCH_3)H(CH_3)]$ complex **5**. The starting point is again complex **14** with a coordinated H_2 molecule. The corresponding TS, $\mathbf{TS_{14\text{-}5}}$, is 48 kJ/mol above **14**. To summarize the reactivity of complex **1m** under hydrogen, the easiest reaction is the formation of the molecular H_2 complex **14** compared to the second grafting. Then, the hydrogenation of the triple bond is much easier than the hydrogenolysis, which yields preferentially **4**. Another important conclusion is that, if the second grafting occurs, it would clearly take place at O-Al_{IV}, which favors for kinetic reasons the pathway

leading to **3',** then **6', 11', 12'**, **13'** and then **2'**. For that reason, only the pathway leading to **2'** has been calculated. Clearly, the second grafting is more activated than other reaction described, and will only happen after these reactions, later in the process.

Figure 4 shows an electronic energy profile, and thermal effects could be important at the typical reaction temperature of 150°C. The main effect would arise due to the loss of entropy for H_2 adsorption, with a corresponding free energy contribution of +50 kJ/mol at 150°C and 1 atm pressure. For the first step, $TS_{1\text{-}14}$, 14, $TS_{14\text{-}5}$, $TS_{14\text{-}4}$, 4 and 5 would be hence destabilized by 50 kJ/mol. The formation of 4 would nevertheless remain most favorable.

For the second reaction step, starting from **4**, the same three reactions are possible, namely the second grafting, the hydrogenation of the double bond and the hydrogenolysis. The second grafting gives $[(Al_sO)_2W(=CHCH_3)H(CH_3)]$ **7** and **7'** with a reaction energy of -45 and -57 kJ/mol, respectively. Contrary to the relative energies of **3** and **3'**, the complex grafted on O-Al_{IV} **7'** is slightly more stable that the one grafted on O-$(Al_V)_2$ **7**. In complex **7**, the hydride is bridged between W and an Al atom with distances of 1.85 and 1.98 Å, respectively. In complex **7'**, the ethylenic H is agostic with a W-H distance of 2.19 Å and a small HCW angle of 90°. The corresponding activation energies are 142 and 104 kJ/mol, through $\mathbf{TS_{4\text{-}7}}$ and $\mathbf{TS_{4\text{-}7'}}$, respectively. Here again, the second grafting on the bridged oxygen is much more difficult than on O-Al_{IV}. Moreover, the second grafting of complex **4** requires slightly larger barriers than that of complex **1**.

The hydrogenation of the double bond in **4** begins, as in the previous hydrogenation of 1, with the molecular coordination of H_2 leading to the complex $[(Al_sO)W(=CHCH_3)(H_2)H(CH_3)_2]$ **15**. This reaction is endothermic by 20 kJ/mol and needs a barrier of 29 kJ/mol. Then the hydrogenation itself leading to complex $[(Al_sO)W(CH_2CH_3)(H)_2(CH_3)_2]$ **8** is exothermic by 31 kJ/mol. The activation energy is 58 kJ/mol through $\mathbf{TS_{15\text{-}8}}$. Hence, the hydrogenation of the double bond is less exothermic and

kinetically somewhat more difficult than that of the triple bond, as it could have been anticipated. To compare with the second grafting reaction, the total barrier from **4** is calculated to be 78 kJ/mol. Starting form **15**, a hydrogenolysis reaction can also occur, leading to complex $[(Al_sO)W(=CHCH_3)(H)_2(CH_3)]$ **9** with elimination of methane. The reaction is exothermic by 64 kJ/mol. In this complex, a strong agostic bond exits with W-H and C-H distances of distances 2.0 and 1.16 Å, respectively and a HCW angle of 79°. The transition state $\mathbf{TS_{15\text{-}9}}$ is 60 kJ/mol less stable than **15**, which gives a total barrier from **4** of 80 kJ/mol, comparable to the barrier of the double bond hydrogenation. Hence, both reactions are equally possible on the potential energy surface. As discussed for step 1, entropy loss from H_2 adsorption destabilize the hydrogenation profile by 50 kJ/mol. In that condition, grafting leading to 7' shows the lowest free energy barrier. In conclusion, starting from **4**, complex 7' will be preferentially formed, corresponding to a second W-O-Al formed with the support.

Further grafting is not possible, since it is sterically difficult to involve more OH groups on the surface starting from 7'. Hydrogenation and hydrogenolysis can continue further, with barriers supposedly equivalent to those found on step 2 (around 80 kJ/mol). Hydrogenation naturally stops after two additions of H_2 on the triple bond, while hydrogenolysis proceeds until all alkyl groups are consumed. This altogether leads to the formation of the complex $[(Al_sO)_2WH_4]$ **13'**, bi-grafted and tetrahydride. For these subsequent steps, reaction energies are all exothermic by 50-60 $kJ.mol^{-1}$ (see Table 1) but the transition states have not been explicitly characterized. As explained above, the formation of **13** is kinetically hindered, since at step 2, the formation of **7'** (implying a terminal OH on an Al_V center) is favored, orienting the reaction in the branch on bi-grafted complexes leading to **13'**.

1m → 3	-83/126	**5 → 9**	-90
1m → 3'	-74/90	**5 → 10**	-22
1m → 14	-9/≈19	**6' → 11'**	-52
14 → 4	-42/2	**7' → 11'**	-64
14 → 5	-15/48	**9 → 11'**	-57
4 → 7	-45/142	**11' → 12'**	-65
4 → 7'	-57/104	**12' → 13'**	-53
4 → 15	+20/29	**13' → 16**	+25/28
15 → 8	-31/58	**16 → 2'**	-51/76
15 → 9	-64/60		

Table 1: Electronic reaction energies / electronic activation energies for the reactions given in Figure 3 (in kJ/mol).

Let us now discuss how the tretrakishydride **13'** leads to the formation of the trihydride **2'**. For this reaction, one hydride has to be removed, which can be performed in the presence of a neighbor proton to eliminate H_2. We have then studied the reaction path shown on Scheme 3, the structure of intermediate **16** and of transition states being given in Figure 7.

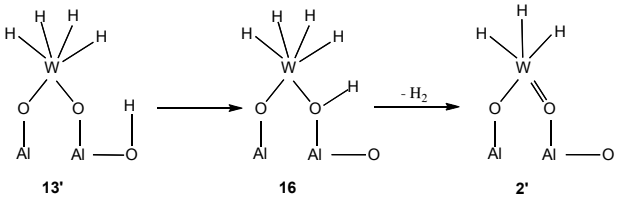

Scheme 3: final reactions steps to form the W trihydride **2'**

With the degree of hydration we have chosen for the alumina surface, corresponding to 3 H_2O per cell, an OH is present close to **13'**, making a hydrogen bond (1.74 Å) with O-Al_{IV} on which W is bound. Even if the hydration degree is lower, there are hydroxyls on the surface coming from the easy hydrogen dissociation on the γ-alumina surface. The migration of this proton to give complex **16** is endothermic (by 25 kJ/mol) and goes through $\mathbf{TS_{13'-16}}$ with a low

barrier of 28 kJ/mol. The elimination of H_2 from **16** is exothermic by -51 kJ/mol and yields **2'** passing via $\mathbf{TS_{16\text{-}2'}}$ with a barrier of 76 kJ/mol. Note that entropic effects would favor H_2 desorption by an extra 50 kJ/mol at 150°C and 1 atm.

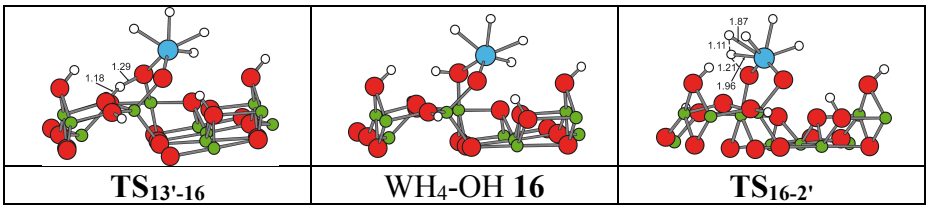

$\mathbf{TS_{13'\text{-}16}}$	WH_4-OH **16**	$\mathbf{TS_{16\text{-}2'}}$

Figure 7- Structures of the transtion states and intermediates involved in the transformation of the tetrahydride $[(Al_sO)_2WH_4]$ **13'** to the trihydride $[(Al_sO)_2WH_3]$ **2'**.

4- Conclusion

In conclusion to the study of this complex network of reactions, the bi-grafted W^{VI} trihydride $(Al_sO)_2WH_3$ **2**, although metastable, is preferentially kinetically formed upon reaction of hydrogen with grafted alkylidyne-alkyl W complex on alumina. Calculated energy barriers are reasonable and can be easily passed over at the reaction temperature (150°C). Among the three involved reactions, namely second grafting, hydrogenation of unsaturated C≡C or C=C bond and hydrogenolysis, the second grafting presents the largest electronic energy barriers (~100 kJ/mol), a value which is still very accessible at the considered temperature. Starting from the initial monografted $[(Al_sO)W(\equiv CCH_3)(CH_3)_2]$ **1m** complex, the most favorable first step is the hydrogenation of the W≡C bond, followed as a second step by the second grafting process, with formation of $[(Al_sO)_2WH(=CHCH_3)(CH_3)]$ **7'**. Performing the grafting on the bridging OH and forming 7 involves an activation energy 38 kJ/mol higher and is hence kinetically hindered. The present results hence explain why the more stable but not reactive W trihydride **2** is not formed, since it would come from intermediate 7. The metastable but reactive W trihydride **2'**, arising from 7', presents a short W-O bond and hence can be described qualitatively as a W-oxo-trihydride in interaction with the alumina surface. Able to

bind ethylene, it is a good candidate for further metathesis reactions. The second grafting step leading to **13**, the tetrahydride precursor of the most stable but unreactive grafted W-hydride **2** is more than 10^4 times slower. Hence the synthesis process favors the formation of the metastable hydride **2'** which is less coordinated by the alumina surface and reactive. The process to form a metastable catalytic structure by grafting and reacting a metallic complex on an oxide support, shown here for the case of W-hydride on alumina, can be seen as good strategy to create active and selective catalysts.

Acknowledgement

The authors are grateful to the Centre Blaise Pascal and the Pôle Scientifique de Modélisation Numérique at the École Normale Supérieure de Lyon for HPC resources.

References

[1] Vidal, V.; Théolier, A.; Thivolle-Cazat, J.; Basset, J.-M. Metathesis of Alkanes Catalyzed by Silica-Supported Transition Metal Hydrides. *Science* **1997**, *276*, 99-102.

[2] Le Roux, E.; Copéret, C.; de Mallmann, A.; Thivolle-Cazat, J.; Basset, J.-M.; Maunders, B. M.; Sunley, G. J. Development of Tungsten-based Heterogeneous Alkane Metathesis Catalysts through a Structure-Activity Relationship. *Angew. Chem. Int. Ed.* **2005**, *44*, 6755-6758.

[3] Taoufik, M.; Le Roux, E.; Thivolle-Cazat, J.; Copéret, C.; Basset, J.-M.; Maunders, B.; Sunley, G. J. Alumina Supported Tungsten Hydrides, new efficient Catalysts for Alkane Metathesis. *Top. Catal.* **2006**, *40*, 65-70.

[4] Basset, J.-M.; Copéret, C.; Soulivong, D.; Taoufik, M.; Thivolle-Cazat, J. Metathesis of Alkanes and Related Reactions. *Acc. Chem. Res.* **2010**, *43*, 323-334.

[5] Mazoyer, E.; Szeto, K. C.; Norsic, S.; Garron, A.; Basset, J.-M.; Nicholas, C. P.; Taoufik, M. Production of Propylene from 1-Butene on Highly Active "Bi-Functional Single Active Site" Catalyst: Tungsten Carbene-Hydride Supported on Alumina. *ACS Catal.* **2011**, *1*, 1643-1646.

[6] Szeto, K. C.; Mazoyer, E.; Merle, N.; Norsic, S.; Basset, J.-M.; Nicholas, C. P.; Taoufik, M. Metallacyclobutane Substitution and Its Effect on Alkene Metathesis for Propylene Production over W–H/Al_2O_3: Case of Isobutene/2-Butene Cross-Metathesis, *ACS Catal.* **2013**, *3*, 2161-2168.

[7] Mazoyer, E.; Szeto, K. C.; Merle, N.; Norsic, S.; Boyron, O.; Basset, J.-M.; Taoufik, M.; Nicholas, C. P. Study of Ethylene/2-Butene cross-Metathesis over W-H/Al_2O_3 for Propylene Production: Effect of the Temperature and Reactant Ratios on the Productivity and Deactivation, *J. Catal.* **2013**, *301*, 1-7.

[8] Mazoyer, E.; Szeto, K. C.; Merle, N.; Thivolle-Cazat, J.; Boyron, O.; Basset, J.-M.; Nicholas, C. P.; Taoufik, M. Insights into the Deactivation Mechanism of Supported Tungsten Hydride on Alumina (W-H/Al2O3) Catalyst for the direct Conversion of Ethylene to Propylene, *J. Mol. Cat. A: Chemical* **2014**, *385*, 125-132.
[9] Joubert, J.; Delbecq, F.; Sautet, P.; Le Roux, E.; Taoufik, M.; Thieuleux, C.; Blanc, F.; Copéret, C.; Thivolle-Cazat, J.; Basset, J.-M. Molecular Understanding of Alumina Supported Single-Site Catalysts by a Combination of Experiment and Theory. *J. Am. Chem. Soc.* **2006**, *128*, 9157-9169.
[10] Maity, N.; Barman, S.; Callens, E.; Samantaray, M. K.; Abou-Hamad, E.; Minenkov, Y.; D'Elia, V.; Hoffman, A. S.; Widdifield, C. M.; Cavallo, L.; Gates, B. C.; Basset, J. M., Controlling the Hydrogenolysis of Silica-Supported Tungsten Pentamethyl leads to a Class of Highly Electron Deficient partially Alkylated Metal Hydrides. *Chem. Sci.* **2016**, *7*, 1558-1568.
[11] Samantaray, M. K.; Callens, E.; Abou-Hamad, E.; Rossini, A. J.; Widdifield, C. M.; Dey, R.; Emsley, L.; Basset, J. M., WMe_6 Tamed by Silica: Si-O-WMe_5 as an Efficient, Well-Defined Species for Alkane Metathesis, Leading to the Observation of a Supported W-Methyl/Methylidyne Species. *J. Am. Chem. Soc.* **2014**, *136*, 1054-1061.
[12] Perdew, J. P.; Wang, Y. Accurate and Simple Analytic Representation of the Electron-Gas Correlation Energy, *Phys. Rev. B* **1992**, *45*, 13244.
[13] Kresse, G.; Furthmüller, Efficient Iterative Schemes for ab initio Total-Energy Calculations using a Plane-Wave Basis Set, *Phys. Rev. B* **1996**, *54*, 11169.
[14] Kresse, G.; Furthmüller, Efficiency of ab-initio Total Energy Calculations for Metals and Semiconductors using a Plane-Wave Basis Set, J. *Comp. Mater. Sci.* **1996**, *6*, 15-50.
[15] Blöchl, P. E. Projector Augmented-Wave Method, *Phys. Rev. B* **1994**, *50*, 17953.
[16] Henkelman, G.; Uberuaga, B. P.; Jónsson, H. A Climbing Image Nudged Elastic Band Method for Finding Saddle Points and Minimum Energy Paths, *J. Chem. Phys.* **2000**, *113*, 9901.
[17] Henkelman, G.; Jónsson, H. Improved Tangent Estimate in the Nudged Elastic Band Method for Finding Minimum Energy Paths and Saddle Points, *J. Chem. Phys.* **2000**, *113*, 9978.
[18] Krokidis, X.; Raybaud, P.; Gobichon, A.E.; Rebours, B.; Euzen, P.; Toulhoat, H. Theoretical Study of the Dehydration Process of Boehmite to γ-Alumina, *J. Phys. Chem. B* **2001**, *105*, 5121-5130.
[19] Digne, M.; Sautet, P.; Raybaud, P.; Euzen, P.; Toulhoat, H. Use of DFT to achieve a rational understanding of acid–basic properties of γ-alumina surfaces. *J. Catal.* **2004**, *226*, 54-68.
[20] Digne, M.; Sautet, P.; Raybaud, P.; Euzen, P.; Toulhoat, H. Hydroxyl Groups on γ-Alumina Surfaces: A DFT Study. *J. Catal.* **2002**, *211*, 1-5.
[21] Joubert, J.; Salameh, A.; Krakoviack, V.; Delbecq, F.; Sautet, P.; Copéret, C; Basset J.M. Heterolytic splitting of H_2 and CH_4 on gamma-alumina as a structural probe for defect sites. *J. Phys. Chem. B* **2006**, 110, 23944-23950.
[22] Zhang, W.; Sun, M.; Prins, R. Multinuclear MAS NMR Identification of Fluorine Species on the Surface of Fluorinated γ-Alumina. *J. Phys. Chem. B* **2002**, *106*, 11805-11809.
[23] Wischert, R.; Copéret, C.; Delbecq, F.; Sautet, P. Optimal Water Coverage on Alumina: a Key to Generate Lewis Acid-Base Pairs Reactive towards the C-H Bond Activation of Methane. *Angew. Chem. Int. Ed*. **2011**, 50, 3202-3205.
[24] Wischert, R.; Laurent, P.; Copéret, C.; Delbecq, F.; Sautet, P. γ–alumina: The Essential and Unexpected Role of Water for the Structure, Stability, and Reactivity of "Defect" Sites. *J. Am. Chem. Soc.* **2012**, *134*, 14430-14449.

[25] Métivier, R.; Leray, I.; Roy-Auberger, M.; Zanier-Szydlowskic, N.; Valeur, B. Characterization of Alumina Surfaces by Fluorescence Spectroscopy. Part 1. Grafting a Pyrene Derivative on γ- and δ-Alumina Supports, *New J. Chem.* **2002**, *26*, 411-415.
[26] Joubert, J.; Delbecq, F.; Copéret, C.; Basset, J.-M.; Sautet, P. Gamma-Alumina: an Active Support to obtain Immobilized Electron Poor Zr Complexes. *Top. Catal.* **2008**, *48*, 114-119.
[27] Listemann, M. L.; Schrock, R. R.; Dewan, J. C.; Kolodziej, R. M. Synthesis and Reactivity of Two Monomeric Tungsten(IV) Phenoxide Complexes. *Inorg. Chem.* **1998**, *27*, 264-271.
[28] Cho, H.G. ; Andrews,L. ; Marsden, C. Infrared Spectra of $CH_3{-}CrH$, $CH_3{-}WH$, CH_2WH_2, and $CH{\vdots}WH_3$ Formed by Activation of CH_4 with Cr and W Atoms. *Inorg. Chem.* **2005**, *44*, 7634-7643